

Source Apportionment of Urban Road Dust Using Four Multivariate Receptor Models

Jithin Jose

Vellore Institute of Technology: VIT University

SRIMURUGANANDAM B (✉ bsrimuruganandam@vit.ac.in)

Vellore Institute of Technology: VIT University <https://orcid.org/0000-0003-1324-5552>

Research Article

Keywords: Road dust, Receptor model, Source apportionment, Resuspended dust, Elemental composition

Posted Date: August 4th, 2021

DOI: <https://doi.org/10.21203/rs.3.rs-163837/v1>

License:   This work is licensed under a Creative Commons Attribution 4.0 International License.

[Read Full License](#)

Source Apportionment of Urban Road Dust using Four Multivariate Receptor Models

Jithin Jose and B. Srimuruganandam *

School of Civil Engineering,
Vellore Institute of Technology,
Vellore – 632 014, Tamil Nadu, India.

E-mail: bsrimuruganandam@vit.ac.in; pauljithinjose@gmail.com

Telephone: 91-416-2202169, Fax: 91-416-2243092.

*Corresponding Author

Abstract

Road dust is one of the biggest contributors to airborne particulate matter (PM) in many urban regions. Due to the inherent heterogeneity of road dust, it is important that its sources are identified and mitigated. Multivariate receptor models are used for source apportionment of PM in many cities. In recent years, these receptor models are finding more applications outside the scope of PM source apportionment. In this study, four multivariate receptor models (Unmix, Positive Matrix Factorization, Principal Component Analysis and Multiple Curve Regression) are used for source apportionment of road dust at Vellore City, India. The elemental composition of road dust samples from 18 locations and for three seasons (summer, winter, and monsoon) are measured using acid digestion followed by Inductively Coupled Plasma - Optical Emission Spectroscopy. Irrespective of models, results showed that crustal material (100% - 68%) and resuspended road dust (82% - 15%) are the biggest contributor to road dust in the study region. Brake wear, tire wear, biomass combustion, vehicular emission and industrial sources are some of the other sources identified by the receptor models. Receptor modeling performance of MCR and PCA models are unsatisfactory. PMF and Unmix models gave acceptable results. From comparing the performance characteristics, Unmix is found to be the ideal receptor model for this dataset. This research clarifies the constraints of different receptor models and the source apportionment information obtained is critical for development of future policy and regulation.

Keywords: Road dust; Receptor model; Source apportionment; Resuspended dust; Elemental composition.

30 **1. Introduction**

31 Chemometric methods of data analysis is a cornerstone for air pollution control in urban
32 environments (Azid et al. 2015). Isolating and quantifying the contribution of various sources to
33 pollution at a location is one of the most common applications of chemometrics in environmental
34 data. This is commonly referred to as receptor modeling (Devi and Yadav 2018). Receptor
35 modeling started gaining popularity during the mid-2000s and continues to be a major player in
36 urban air quality management (Zhang et al. 2017). These models reconstruct the contribution of
37 individual sources to pollution in a region using the ambient pollutant concentration information
38 (Henry et. al., 1984) and are frequently used for source apportionment of particulate matter (PM)
39 emissions (Heo et al. 2009).

40 Road dust is consistently seen in source apportionment studies irrespective of study location
41 (Belis et al. 2014). Road dust is the loose, mostly crustal material settled in road surfaces that is
42 resuspended by the action of wind or wake from vehicular movement (Abu-Allaban et al. 2003;
43 Amato et al. 2009). Combustion and non-combustion vehicular emissions such as exhaust
44 emissions, tire wear, brake wear and engine wear are the common source of road dust in urban
45 environment (Denby et al. 2018). Non-vehicular sources of road dust include crustal material
46 transported by wind (Mao et al. 2013), construction and demolition activities (Marín et al. 2011)
47 and street sweeping (Amato et al. 2010). The heterogenous nature of road dust impacts human
48 health necessitating effective qualitative and quantitative apportionment of the sources. This
49 information is needed to develop effective control and mitigation strategies to reduce morbidity
50 from exposure to road dust (Bartkowiak et al. 2017).

51 Toxicological studies have noted that these sources of road dust can release dangerously high
52 amounts of potentially toxic elements (PTEs) (Arslan 2001) and polycyclic aromatic hydrocarbons

53 (PAH) (Khpalwak et al. 2019). Many of these chemicals are also classified as “probably
54 carcinogenic to humans” by the International Agency for Research on Cancer (IARC 2020).
55 Studies show that children are at a greater risk of being exposed to high concentration of PTEs and
56 PAH since they spend a greater portion of their day outdoors (Zeng et al. 2019). Developmental
57 disorders like impaired mental development (Isaac et al. 2012) and stunted growth (Zeng et al.
58 2019) are common in children exposed to elevated concentrations of PTEs.

59 Source apportionment of PM is studied extensively in research from around the world
60 (Banerjee et al. 2015). However, application of these receptor models in source apportionment of
61 road dust have garnered considerably less attention. Cities in developing countries tend to see even
62 fewer studies. This is alarming because many of the world’s most polluted cities are in developing
63 countries, especially in South Asia. Vellore is a small tier - 2 city (MHRD 2015) in the South
64 Indian state of Tamil Nadu. The city is spread over a land area of 87.92 km² and has a population
65 of 177,230 (as per 2011 Census). For a semi-arid land locked city like Vellore, road dust is a major
66 cause of concern. In this study, the results from four receptor models are compared viz., Unmix,
67 Positive Matrix Factorization (PMF), Principal Component Analysis – Multiple Liner Regression
68 Analysis (PCA-MLRA), and Multiple Curve Regression – Alternating Least Squares (MCR-ALS).
69 The major objectives of this study are, (1) Identifying and apportioning the sources of road dust in
70 the city, thereby helping future endeavors in regulation and policy, (2) Recognizing the constraints
71 of different receptor models used in this study, and (3) Most importantly, this research could prove
72 to be instrumental in reinvigorating receptor modeling studies on road dust.

73 **2. Methodology**

74 **2.1. Sample Collection and Analysis**

75 Figure 1 shows the sampling region and sampling locations. Deposited dust samples from the road
76 surface are collected from 18 locations within Vellore City. Table 1 shows the various sampling
77 locations. More information on the sampling region is explained in Jose and Srimuruganandam
78 (2020). Road dust samples are collected from 27th and 28th of January 7th and 8th April and 22nd
79 and 23rd May of 2018 corresponding to Winter, Summer and Monsoon Seasons. Vellore city does
80 receive summer rains towards the end of May and early June. The samples for monsoon season
81 are collected towards the end of May a proxy for monsoon season since rains are unceasing during
82 monsoon season, which makes it nearly impossible to collect samples. The samples for monsoon
83 season were collected after two weeks of sporadic rains. Approximate weights of the samples were
84 taken in situ using a generic weighing balance. The weighed samples are then sieved manually as
85 per ASTM C136 (ASTM 2001). The portion of the sample that passed through 75 μ m sieve is
86 subjected to microwave digestion using a mixture of HCl and HNO₃ as per U.S.EPA 3050b
87 procedure (U.S. EPA 1996) for direct energy coupling devices. The digested samples are analyzed
88 for 25 elements (Ag, Al, As, Ba, Bi, Ca, Cd, Co, Cr, Cu, Fe, Ga, In, K, Li, Mg, Mn, Na, Ni, Pb,
89 Rb, Se, Sr, Tl, Zn) by Inductively Coupled Plasma - Optical Emission Spectroscopy (Perkin Elmer,
90 Avio - 200). Detailed information on sample collection, sample analysis and quality control can
91 be found in Jose and Srimuruganandam (2020).

92 **[INSERT FIGURE 1]**

93 **[INSERT TABLE 1]**

94 **2.2. Multivariate Analysis**

95 In this study, the efficacy of four different multivariate receptor models for source apportionment
96 of road dust are examined viz., PCA-MLRA, Unmix, MCR-ALS, and PMF.

97 PMF model is performed using pre-compiled binary available for Microsoft® Windows
98 operating system from U.S. EPA. EPA-PMF v.5.0 is used for this study. The software is run atop
99 Microsoft® Windows 10 (OS build 18363.836).

100 Pre-compiled binary for Unmix is available for Microsoft® Windows operating system from
101 U.S.EPA. EPA-Unmix v.6.0 is used for this study. Since this binary is incompatible with modern
102 operating systems, it is run in an Oracle VirtualBox virtual machine instance (1 logical processor
103 and 1 GB RAM) on Microsoft® Windows XP (SP3).

104 MCR-ALS is performed using R, an open-source statistical modeling package (v.3.6.2)
105 coupled with RStudio (v. 1.2.5) interactive development environment (IDE). ALS library available
106 from the Comprehensive R Archive Network (CRAN) repository is used in this model.

107 Like MCR-ALS method, PCA-MLRA is done using R, (v.3.6.2) coupled with RStudio (v.
108 1.2.5) IDE. PCA and MLRA are done using functions available by default in R (prcomp and lm).

109 All receptor modelling processes in this study are performed on a ThinkPad T430 Personal
110 Computer (Intel Core i5- 3320M 2.60GHz, 8GB RAM). A brief explanation on various
111 multivariate receptor models used in this study is given below.

112 **3. Theory of Receptor Modeling**

113 Receptor models are mathematical model that are used to identify and quantify the contribution of
114 different sources of a pollutant at a receptor location. These models use the chemical composition
115 of a pollutant at a receptor location to identify its sources. This is in stark contrast to source-
116 oriented models where the concentration at a receptor location is estimated if the properties of the
117 source and meteorological conditions are known. The major advantage of using receptor model is
118 that they use real measured ambient pollutant concentrations.

119 Most receptor models work by factoring a large concentration data matrix into two lower rank
120 matrices. Since the number of samples are always greater than the number of variables, these
121 equations cannot be solved uniquely. Receptor models are used to obtain the best possible solution.
122 The difference between receptor models depends largely on the various approaches and constraints
123 employed by these models to get a valid solution (Henry 1991). Since the value of concentration
124 cannot be negative, non-negativity of mass concentration is a constraint used consistently in
125 receptor models (Belis et al., 2014). However, non-negativity alone is seldom enough for a
126 complete solution. Many other constraints are considered in modern receptor models like;
127 measurement uncertainty, factor rotation and multi-dimensional edge detection (Pant and Harrison
128 2012). In this study, source apportionment of road dust collected from Vellore city of South India
129 is studied by using different multivariate receptor models.

130 Meta-analysis of source apportionment conducted all over Europe show that the number of
131 receptor modelling studies is more than all other source apportionments methods combined (Belis
132 et al. 2014). Compared to other source apportionment methods, the location-first approach of
133 receptor modeling makes them ideal to assess the compliance of a receptor location to air quality
134 limits. Receptor-oriented models do not consider complex chemical and meteorological processes.
135 These models therefore have very modest computational requirements compared to source-
136 oriented models. Multivariate receptor models also negate the need for emission inventories thus
137 reducing uncertainties related to it (Hopke 2016). The inability of model reactive species limits the
138 use of receptor models to regional or urban scale. Application of receptor models necessitates the
139 availability of quantitative data at the receptor and demands good knowledge of the atmospheric
140 conditions and chemical nature of sources from the researcher.

141 It is hard to establish a minimum number of samples in advance, since that number would
 142 be dependent on the amount of information within the data set (Belis et al. 2014). Studies show
 143 that at least 50 chemically characterized samples are needed to run multivariate analysis. (Johnson
 144 et al., 2011). Other studies also mention that the number of samples should be approximately three
 145 times the number of variables (Thurston & Spengler, 1985). Also, small datasets from multiple
 146 sites in a region are used in previous source apportionment studies (Xie et al., 2012). All
 147 multivariate factor analysis works on the principle of matrix factorization (Hopke 2016). This can
 148 be expressed mathematically by the expression.

$$149 \quad C_{(m \times n)} = G_{(m \times p)} \times F_{(n \times p)}^T + E_{(m \times n)} \quad (1)$$

150 where, the matrix C is the concentration of n elements collected at m locations, F is the factor
 151 matrix with n elements and p factors, G is the mass concentration matrix with m observations and
 152 p factors. The matrix E has information on the residuals from the model caused due to experimental
 153 and measurement errors. Different receptor models apply different constraints to F and G matrices
 154 to minimize the residuals in the E matrix.

155 **3.1. Unmix**

156 The Unmix method is a multivariate model with built-in non-negative constraints. It begins with
 157 singular variable decomposition (SVD) of the concentration matrix C and is represented by the
 158 equation below (Henry 2003).

$$159 \quad C_{ij} = \sum_{i=1}^p \sum_{k=1}^p U_{ik} D_{kl} V_{lj} + E_{ij} \quad (2)$$

160 where C_{ij} is the input data, U and V are orthogonal $n \times n$ and $m \times m$ matrices. D is an $n \times m$
 161 diagonal matrix. The Unmix model uses SVD to find the edges in an m -dimensional data space
 162 and reduce the dimensionality of data from m to N , where n is the number of sources identified.

163 Equation 2 is like the general receptor model equation (Equation 1). The exception is that in normal
164 chemical mass balance approach, source composition is already known.

165 One of the major advantages of using Unmix model is that it has the non-negativity criteria
166 build into model. This negates problems arising from negative mass concentrations. Also, since
167 this model extracts all required constrains to solve the chemical mass balance equation from the
168 data itself, measurement uncertainties are not required to run this model. However, since the model
169 uses eigen vector analysis, it is not well suited for heteroskedastic data commonly seen in
170 atmospheric modeling.

171 **3.2. PCA**

172 PCA is an eigen vector method of matrix factorization that is used to reduce many possibly
173 correlated variables into a smaller number of uncorrelated principal components. In PCA method,
174 the total concentration of each element i is assumed to be a sum of the elemental contribution from
175 the different elemental sources j . Thus, a normalized concentration matrix can be written as,

$$176 \quad Z_{ik} = \sum_p^{j=1} W_{ij} P_{jp} \quad (3)$$

177 Equation 2 can be rewritten in matrix terms as an analogue to equation 1 as,

$$178 \quad [P]_{j \times \lambda} = [B]_{j \times i} [Z]_{i \times \lambda} \quad (4)$$

179 This equation (3) is now equivalent to equation (1). The matrix $[P]_{j \times i}$ is factorized based on
180 eigen value decomposition. Absolute Principal Component Scores are calculated by subtracting
181 an absolute zero principal component matrix from $[P]_{j \times i}$ matrix as shown in equation (4) (Thurston
182 and Spengler 1985).

$$183 \quad [APCS]_{p \times j}^* = [P]_{p \times j}^* - [P_o]_{p \times j}^* \quad (5)$$

184 Later, mass distribution for each day is calculated by multiple linear regression analysis of
185 the APCS to total mass for each day as shown in equation (5).

$$186 \quad M_k = \zeta_0 + \sum_{j=1}^p \zeta_j APCS_{jk}^* \quad (6)$$

187 Like Unmix, PCA model extracts all required constrains to solve the chemical mass balance
188 equation from the data itself, measurement uncertainties are hence not used in this model. Also,
189 PCA method does not require any specialized software. Many commercially available and open-
190 source statistical packages have PCA model build into them. PCA is also an eigen vector
191 decomposition method. Hence, the problems with heteroskedastic data haunts PCA. Unlike
192 Unmix, PCA has no build in non-negativity constraints. This omission can lead to presence of
193 negative mass concentration in source apportionment results. Although, PCA is generally not
194 recommended for quantitative source apportionment, they can be used effectively for exploratory
195 analysis.

196 **3.3. MCR**

197 MCR-ALS is a method used to recover pure response profiles of chemical components from an
198 unresolved mixture without prior knowledge of its composition. This method is initially developed
199 for gas chromatographs. However, this source apportionment is also a matrix factorization
200 problem, MCR-ALS algorithm can be used. In the MCR-ALS model, the matrices G and F in
201 equation (1) is calculated by minimizing the sum of squared residuals SSR (Tauler et al. 2009).

$$202 \quad SSR = \sum_{i=1}^m \sum_{j=1}^n (x_{ij} - \bar{x}_{ij})^2 \quad (7)$$

203 In equation (6), x_{ij} is the measurement of j^{th} element in the i^{th} sample. Although this algorithm
204 can work when both matrices are unknown, the problem can be further simplified by finding an

205 initial solution using a simpler algorithm like simple-to-use interactive self-modeling analysis
206 (SIMPLISMA). Once matrix F is initialized, matrix G is calculated using:

$$207 \quad G = XF(F^T F)^{-1} \quad (8)$$

208 Non negativity in G is obtained by minimizing the sum of residuals in matrix X such that all
209 elements in matrix G is greater than zero. This G is then used to recalculate F using:

$$210 \quad F^T = (G^T G)^{-1} G^T X \quad (9)$$

211 This iterative procedure continues until SSR value from two consecutive iterations fall below
212 a preset value.

213 Unlike PCA and Unmix model, MCR model use alternating least squares for solving the
214 chemical mass balance equation. Hence, this model is well suited for use in applications where
215 heteroskedastic data is analyzed. This model also has the advantage that non-negativity criteria is
216 built into it. All these advantages come at the cost of slightly higher computational requirements.

217 **3.4. PMF**

218 PMF is a purpose made receptor model that is developed by U.S. EPA for source apportionment
219 applications. The general working of PMF model is like MCR-ALS model with the exception that
220 the sum of squares of residuals SSR is minimized using the equation (Paatero and Tapper 1994):

$$221 \quad SSR = \sum_{i=1}^n \sum_{j=1}^m \left[\frac{X_{ij} - \sum_{k=1}^p G_{ik} \cdot F_{kj}}{u_{ij}} \right]^2 \quad (10)$$

222 Like MCR-ALS model, PMF model is more suited for heteroskedastic data since it allows
223 individual weighing of data points. Usually, this model tends to resolve more sources than the

224 other models tested here. The downside of this model is that it requires considerably higher
225 computational requirements compared to the other models.

226 **4. Results and Discussion**

227 Source apportionment is performed using the chemical composition of the collected silt samples
228 (fraction of road dust with size $<75\mu\text{m}$). Silt component of road dust is highest during the summer
229 season with 160g for 1kg of sample tested. This is followed by winter (152.2g) and monsoon
230 season (108.4g). The highest fraction of silt in road dust sample is at location 7, near Vellore
231 district administrative office (264g). Being an administrative center, this location experiences
232 considerable vehicular traffic. The sampling location is also located below an overpass thus
233 impeding air movement. Lowest silt fraction is at location 1 (88.37g) since this road has paved
234 sidewalks and is cleaned regularly. More information on chemical composition of analyzed road
235 dust and its seasonal variations is explained in Jose and Srimuruganandam (2020).

236 A total of six sources are identified by the four receptor models, viz., crustal material,
237 resuspended dust, tire and brake wear, biomass combustion, industrial sources, and vehicular
238 emission. Source apportionment by the individual receptor models is explained in more detail
239 below. It is to be noted that the sources are numbered for identification only and are not ranked in
240 by any means.

241 **4.1. Unmix**

242 For the Unmix model, 51 of the 52 observations are taken for consideration. One observation is
243 ignored (location 14 during winter season) to improve signal to noise ratio of the data. 100 feasible
244 solutions for unmix model are obtained from 218 runs. Run number 15 is chosen as the global
245 minima. The model identified five sources with a minimum R^2 value of 0.93 and a minimum signal

246 to noise ratio of 1.91. Source contribution of the five sources to different elements is shown in and
247 their contribution to different sources with different sampling locations is shown in Figure 2. The
248 scaled residuals are found to be between -3 and +3.

249 **[INSERT FIGURE 2]**

250 *4.1.1. Source 1: Resuspended Dust*

251 The first source accounts for all the Pb present in road dust of Vellore city. It also shows significant
252 contributions to nearly all elements. It contributes least to K (5%), Mg (5%), Mn (8%), and Sr
253 (8%). Low contribution to K would rule out biomass combustion as this source. High contribution
254 to Pb (100%), Rb (22%) and Li (21%) suggests that this source could be resuspended road dust.
255 The probable source of Pb in this fraction could be from automobile exhaust prior to the year 2000;
256 when leaded fuel was banned in the country (Miguel et al. 1999; Das et al. 2018). Since lead halide
257 salts from vehicle exhausts are largely insoluble, they tend to remain in the environment for a long
258 time (Habibi 1970). From Figure 2, it is visible that the contribution of this source to pollution is
259 considerably high during the summer season. The semi-arid summers in the region are the reason
260 for increased resuspension of road dust. Winter season shows a relatively consistent contribution
261 of this source throughout the study region. However, there are clearly defined hotspots during
262 summer and monsoon. Highways are the most obvious hotspots of this source as evident from
263 locations 6, 8, 9 and 10. However the presence of Pb in location 14 can have other sources since
264 lead-acid battery refurbishment shops operate regularly in this region (Jose and Srimuruganandam
265 2020).

266 *4.1.2. Source 2: Crustal Material*

267 Second source of road dust identified by Unmix shows significant contributions to almost all
268 elements in the study region. With high contributions going to Al (50%), Ba (82%), Zn (71%), Mg
269 (71%), Sr (74%) and Co (55%). This source is expected to be a combination of both tire wear and
270 biomass combustion. High contribution to K and Mg show that biomass combustion could be a
271 contributor to this source (Pio et al. 2008). All other elements with high contribution from this
272 source suggest that tire wear is also a contribution to this source. Zn is a common tracer that is
273 used for identifying contamination from tire wear (Kupiainen et al. 2005). Studies have shown that
274 up to 1% of the tire tread material can be Zn (Councell et al. 2004). Co is added to the rubber
275 matrix to promote its adhesive characteristics (Fulton 2005), thereby improving the strength of tire
276 compound (Ooij 1984). Fluoride salts of Sr are used in some tire formulations for improving the
277 stability of resins (Yasuda et al. 1990). Magnesium alloys and forged aluminum are both used in
278 manufacture of engine blocks and pistons implying presence of engine wear in this source
279 (Lakshminarayanan and Nayak 2011).

280 This source is found to contribute heavily to road dust in locations 3, 17 and 18. This is
281 essentially a long stretch of road and thus tire wear can be a significant source of pollution in these
282 locations. Locations 3 and 18 are adjacent to gas stations. Barium from diesel fuel additives and
283 engine oil additives can also be contributing to the high levels of this source in these locations
284 (Monaci and Bargagli 1997). There is a considerable seasonal variation of this source. Winter
285 season shows the highest contribution whereas the monsoon season shows the lowest contribution.

286 *4.1.3. Source 3: Break Wear*

287 The third source shows high contribution to Fe (27%) along with a significant contribution to Al
288 (7%), Li (14%) and Cu (8%) suggests that break wear can be a contributor to this source (Gramstat
289 2018). High contribution to Fe can be attributed to wear from brake disks and drums used in

290 automotive braking systems (Garg et al. 2000; Kukutschová and Filip 2018). This source shows
291 high contribution throughout all three seasons. The highest contribution is noted during the
292 summer season. Winter season also shows a similar distribution for this source. Lowest
293 contribution for this source is noted during monsoon season since the brake dust could be washed
294 off during monsoons. Considerable spatial variation is not exhibited by this source.

295 *4.1.4. Source 4: Vehicular Emissions*

296 Fourth source shows significant contribution to Cr (66%), Ni (58%), Mn (47%), Ga (45%) and Cu
297 (48%). This suggests that the fourth source of road dust is possibly from vehicular emissions.
298 Source apportionment studies generally consider Ni as an indicator for oil combustion (Thomaidis
299 et al. 2003; Peltier et al. 2009). Studies show that heavy duty diesel engines can release significant
300 quantities of Mn (Hilden and Bergin 1986) and Cu (Konstandopoulos et al. 1988) since they are
301 used as fuel additives. Cr coating is used in high power diesel engine piston rings to prevent wear
302 (Rastegar and Craft 1993). Traces of these elements are also usually present in engine oils used by
303 diesel engines. From Figure 2 contribution of this source to road dust is maximum during the
304 summer season. Winter and monsoon show nearly equal distribution throughout the study region.

305 *4.1.5. Source 5: Crustal Material*

306 Fifth source shows high contribution only to Fe (19%). Since Fe is one of the most abundant
307 elements on earth's crust (Turekian and Wedepohl 1961; Taylor 1964), it can be assumed that the
308 fifth source of road dust is crustal material. From Figure 2, contribution of crustal material to road
309 dust is minimal during the summer since vehicular emission and tire wear take a more prominent
310 place during this season. This source contributes high during the monsoon season. Rains during
311 monsoon season are expected to wash away pollutants from other sources.

312 4.2. PMF

313 Microsoft Windows binary for EPA PMF 5.0 provided by U.S.EPA is used for the PMF model.
314 Of the 52 samples, 14 samples are discarded to improve the signal to noise ratio of the model
315 (shown as empty circles in Figure 3). The number of bootstrap runs is kept 100 with a minimum
316 r^2 of 0.6. The Q-robust of the model is found to be close to Q-true, suggesting that results are
317 acceptable. Scaled residuals for this model is between -7 and 7.

318 **[INSERT FIGURE 3]**

319 4.2.1. Source 1: Vehicular Emission

320 First source shows high loading only for Ba (57%). It is also seen to contribute moderately to Co,
321 Sr, Mg and Zn. The high loading of Ba indicates that this source could be vehicular emission.
322 Studies have shown that Ba is an effective indicator for vehicular emission (Monaci and Bargagli
323 1997; Monaci et al. 2000). Barium fuel additives are used extensively in diesel engines to reduce
324 smoke from combustion (Glover 1966; Truex et al. 1980). Barium fluoride is also used in some
325 engine oils to improve its load carrying capacity (Hermant et al. 1986). Monsoon season shows
326 the highest contribution from this source (Figure 3) since other sources of road dust could have
327 been washed away. Location 17 shows extremely high contribution during winter season.
328 Similarly, high contribution was also identified by Unmix model (Figure 2). This could be an
329 isolated incident like an oil spill.

330 4.2.2. Source 2: Biomass Combustion

331 Second source shows a high contribution towards K. This is indicative that this source could be
332 from biomass combustion. Potassium (Andreae 1983) and Levoglucosan (Achad et al. 2018) are
333 the two most common indicators for biomass combustion. This source shows higher contribution

334 to road dust during the summer season due to the increased biomass load present in the road
335 surfaces. As expected, contribution from this source is found to be higher during summer season
336 and least during monsoon season (Figure 3). Contribution from this source is negligible during
337 monsoon season since damp vegetation inhibits combustion.

338 *4.2.3. Source 3: Resuspended Road Dust*

339 The third source shows considerable contribution to Pb (71%), Ni (24%) and Cr (25%). It also
340 contributes to most other elements that are analyzed. High contribution to Pb would suggest that
341 this source is re-suspended road dust (Al-Chalabi and Hawker 1997; Wang et al. 2005). As stated
342 before, Pb based antiknock agents have been phased out of the country since 2000 (Sharma and
343 Pervez 2003). So, the contribution to Pb by this source can only be attributed to previously
344 deposited Pb two decades ago. As noted in the unmix model, the contribution of this source to road
345 dust in the region is greater during summer season due to the semi-arid conditions that are prevalent
346 in the city during summer.

347 *4.3.4. Source 4: Tire and Brake Wear*

348 Fourth source shows high concentration to Cu (54%), Zn (29%), Cr (44%), and Ni (50%). Zinc is
349 an indicator for tire wear (Wang et al. 2005) and copper is seen more in brake wear particles
350 (Thorpe and Harrison 2008). As mentioned in previous models, Ni is an indicator for oil
351 combustion (Galbreath et al. 2000) and Cr can be linked to vehicular exhaust (Testa 2004). This
352 source can hence be concluded to be vehicular emission. From Figure 3 the contribution of this
353 source to the road dust in this region is greater towards the city center compared to the outskirts.
354 The increased traffic at this location can be the reason for this observation. Mean contribution from
355 this source is found to be greater during the winter season. Although tire wear generally increases

356 during the summer season due to higher road temperature, the higher emissions from vehicle
357 exhausts and brake wear could have offset this.

358 *4.2.5. Source 5: Crustal Material*

359 The final source of road dust identified by PMF shows high contribution to Al (39%), Ca (42%),
360 Fe (44%), Mg (38%), Sr (44%) and Co (53%). Fe, Ca, and Al are the most abundant elements in
361 the earth's crust (Yaroshevsky 2006) suggesting that the fifth source is crustal material. This source
362 is found to contribute more to road dust during the winter season. The lowest concentration of road
363 dust is identified at the bridge across river Palar (Location no. 4). Higher contribution of sources
364 like tire and brake wear during summer season decreases the percentage contribution of crustal
365 material during summer season. Lower road temperatures during monsoon season coupled with
366 rains washing off smaller dust particles could be reason for high contribution of crustal material
367 (Figure 3).

368 **4.3. PCA-MLRA**

369 PCA model is run using a custom R script. All 52 samples are used in this model. Kaiser-Meyer-
370 Olkin (KMO) measure of sampling adequacy is 0.56 for the collected data. This suggests a factor
371 analysis can be performed with the data. Bartlett's test gave a significance level considerably lower
372 than 0.05 suggesting that the variables are related, and factor analysis can provide useful
373 information. Both the tests were performed using KMO and Bartlett test functions in 'psych'
374 library available at CRAN. With a cut off eigen value of 1, PCA can extract 5 principal components
375 (Table 2). The five principal components extracted accounted to 85% of the total variance.

376 **[INSERT FIGURE 4]**

377 *4.3.1. Source 1: Crustal Material*

378 The first principal component accounts for 25% of the total variance explained by PCA. This
379 component shows high loading for Al, Sr, Mg, Cr, Fe and Mn. The major source of these elements
380 in road dust is from crustal matter. Al and Fe are two of the most abundant elements present on
381 earth's crust (Rudnick et al. 2019). This source is found to contribute significantly to road dust in
382 the region throughout the year especially during the summer season (Figure 4). The dry summers
383 in the study region can be contributing to this. Major hot spots for this source are along roads that
384 lack a paved sidewalk or hard shoulders.

385 *4.3.2. Source 2: Biomass Combustion*

386 Second principal component accounts for 18% of the total variance and shows high loading for K
387 and Li. High loading for K indicates presence of biomass (Yu et al. 2018). Hot spots for this source,
388 largely concentrated along Gandhinagar main road (locations 2, 3, 17 and 18) show that biomass
389 combustion has a higher contribution during monsoon season. This anomaly could be because
390 other sources could also be included in this principal component. Previous studies have noted the
391 presence of an unidentified source of Li in this region (Jose and Srimuruganandam 2020).
392 Locations towards the south of the city show contribution from this source during monsoon season,
393 which is in stark contrast to PMF model, where contribution from biomass combustion is largely
394 absent during this season.

395 *4.3.3. Source 3: Resuspended Dust*

396 Third component shows high loading for Mg, Sr, Cr, Cu, Ni and Pb. This source accounts for 16%
397 of total variance and contribute more during the winter season. High loading for Pb suggests that
398 the third source is from re-suspended road dust. Two of the biggest hot spots of re-suspended road

399 dust according to PCA-MLRA are Palar river bridge (location 4) and highway underpass (location
400 15).

401 *4.3.4. Source 4: Crustal Material*

402 Fourth principal component also shows high loading for Ca and Fe. Suggesting that this source is
403 also crustal in origin. This source contributes more to road dust during the winter season, with
404 contributions greater towards the south of city, suggesting that contribution from resuspended dust
405 might also be accounted in this source (Figure 2). This source has negligible contribution to road
406 dust during summer and monsoon seasons.

407 *4.3.5. Source 5: Tire Wear*

408 Fifth principal component accounts for 8% of the total variance. This component shows high
409 loading for Ba, Cu and Zn. High loading for Zn and Cu suggests that the source is likely from tire
410 wear (Kupiainen et al. 2005). Ba is usually present in vehicular emissions. The presence of Ba in
411 suggests that this source could be a combination of both tire wear and vehicular emissions. This
412 source has exceptionally low spatial variation and is distributed equally throughout the study
413 region. As seen in Unmix and PCA models, contribution is higher during summer season and least
414 during monsoon season (Figure 4). High vehicular traffic combined with impeded ventilation
415 could be the reason for higher contribution of this source in location 7 (Figure 4).

416 **4.4. MCR-ALS**

417 The MCR-ALS model is run using the 'ALS' library provided by CRAN. For running the MCR
418 model, an initial solution is necessary. This solution will help in reducing the number of iterations
419 necessary before reaching a satisfactory solution. Since the SIMPLISMA model did not have an
420 equivalent under CRAN, the results from the PCA model are used as an initial solution for the

421 MCR-ALS model. The model converged in 14 iterations with non-negativity criteria for both
422 matrices. This model could extract only three sources from the receptor concentration data. The
423 deviation of data from ideal bilinear behavior can be the reason for poor source apportionment
424 results. The initial differential residual (RD) is 0.85. After 14 iterations alternating between
425 optimizing S and C matrices, the RD value dropped below the default threshold of 0.001. The
426 scaled residual in this model lies below ± 3 .

427 **[INSERT FIGURE 5]**

428 *4.4.1. Source 1: Industrial Source*

429 The first source shows contribution to Al and Mg. Presence of this source close to location 17
430 suggests that this source could be of industrial origin. There is an industrial estate towards east of
431 location 17 which can contribute to pollutants in this location. This source has a higher contribution
432 during summer and least contribution during monsoon season (Figure 5). Summer season shows
433 high contribution of this source in locations 1, 2, 4, 5 and 7. Winter contribution is greater at
434 locations 2, 7 and 17. Contribution from this source must be studied further by dispersion modeling
435 methods.

436 *4.4.2. Source 2: Crustal Material*

437 Second source contributes to the entirety of Fe, Li and K. It also shows significant contribution to
438 Ca, Ga, Ni, Na and Sr. Presence of high contributions to Ca and Fe would suggest that this source
439 is of crustal origin. As discussed in previous models, the mean contribution of this source to road
440 dust is greater during monsoon season due to wash off soil from sidewalks. Other sources like
441 brake wear and tire wear are washed away by rains during the summer where re-suspended dust is

442 found to contribute more. Contribution from this source is least during summer season due to
443 contribution from resuspended dust and tire and brake wear as seen in Figure 5.

444 *4.3.3. Source 3: Resuspended Dust*

445 This source is found to contribute more to Pb, Rb, Zn, Cr, Co, and Al. Presence of these elements
446 suggests that this source is largely from re-suspended road dust. Like other models in this study,
447 contribution from this source is greater during summer season. MCR model shows no contribution
448 from this source during winter season. Contribution from this source is found to be greater at
449 locations that lack a paved sidewalk (Figure 5).

450 **4.5. Seasonal Variation of Sources**

451 Unmix, PMF and MCR-ALS models show that contribution of crustal materials to road dust is
452 found to be greater during monsoon season. Only PCA-MLRA model shows higher contribution
453 during summer season. Considering that PCA-MLRA model overestimates the contribution of this
454 single source considerably, the results obtained from it can be erroneous. The other three models
455 attribute lowest contribution to summer season. As mentioned in previous sections, this can be
456 attributed to increased tire and brake wear during summer season.

457 High contribution of resuspended road dust during summer season is identified by all four
458 models. Drier road conditions during summer season can lead to increased resuspension of road
459 dust particles. Likewise, all four models identified that the contribution of resuspended road dust
460 is least during monsoon season owing to the wet deposition of resuspended dust when in contact
461 with rains.

462 Contribution of tire and brake wear is found to be nearly equal during summer and winter
463 seasons and lowest during monsoon seasons. Summer contribution is slightly higher due to

464 increase in tire wear resulting from the higher road temperatures. Winter contributions are equally
465 high due to stable atmospheric conditions that are observed during winter months. Tire and brake
466 wear particles tend to be very small and hence can be easily washed away. This would explain the
467 low concentration during monsoon season.

468 Unmix is the only model that could identify contribution from vehicular emissions. This
469 source shows high contribution during summer season. Winter and monsoon concentrations are
470 nearly equal. Biomass combustion on the other hand have contradicting results from two models.
471 PMF model shows high contribution of biomass burning during summer season. This is the
472 expected result since biomass combustion is highly unlikely during monsoon season. However,
473 this anomaly is observed in PCA-MLRA. Presence of elements like Li and In in this source
474 suggests that the specific principal component is a combination of sources.

475 **4.6. Spatial Distribution of Sources**

476 The models identified six sources in total: crustal matter, re-suspended road dust, biomass combustion, tire
477 and brake wear, vehicular emission and industrial. Of these sources, crustal matter and re-suspended road
478 dust is identified by all the models. Tire wear, brake wear or a combination of both is identified by three
479 models (Unmix, PCA and PMF). Two models (PCA and PMF) identified biomass as a source of pollution
480 in the region. Industrial source is identified by MCR-ALS model and vehicular emission is identified by
481 Unmix model. The spatial distribution of various sources quantified by the source apportionment models
482 are shown in Figure 6.

483 **[INSERT FIGURE 6]**

484 Crustal source is identified by all four receptor models. The PCA model placed the highest
485 contribution on crustal source. Lowest contribution is apportioned by the PMF model. The PCA model
486 shows exceptionally low spatial variance in this source. The contribution of this source is found to vary

487 from 84% to 94%. Unmix model shows slightly higher spatial variance in source contribution from crustal
488 matter (37% to 62%). Hot spots identified are along the main road (locations 15 and 16). The PMF model
489 also shows similar hot spots. The contribution of crustal material according to the PMF model is
490 considerably low compared to other models. MCR model showed the highest variance in contribution from
491 this source (between 65% and 100%). From Figure 3 and Figure 4, both PMF and Unmix models show
492 high contribution from crustal material during monsoon season. Higher contribution is noted in roads that
493 lack a paved sidewalk (locations 9, 10 and 13).

494 Re-suspended road dust is another source identified by all four receptor models. The contribution of
495 resuspended road dust is estimated to be between 1% and 16%. Highest contribution to the source is
496 estimated by the PMF model. As per the PMF model, the contributions varied from 2% to 23%. The highest
497 contributions are noted at highways (locations 6 and 8). Lowest contribution is noted at Gandhinagar main
498 road (location 17). Unmix model also identified location 8 as a hotspot for this source. Lowest mean
499 contribution is obtained from the PCA model. Three of the four models show highest contribution from
500 resuspended road dust during summer and lowest contribution during winter (Figures 2, 3 and 5). PCA
501 apportioned the least contribution from resuspended dust during summer season. Figure 4 shows that PCA
502 overestimated the contribution from crustal material in all three seasons.

503 Unmix model shows relatively high contribution for tire and brake wear (17% to 44%). Lowest
504 contribution to this source is noted by the PCA model. Unmix and PMF models show high contribution of
505 tire and brake wear during summer season and lowest during monsoon season (Figure 2 and 3). Biomass
506 combustion is identified by both PCA and PMF models. PMF model shows higher contribution for this
507 source during summer season. PMF model apportioned negligible contribution from this source during
508 monsoon season while PCA model apportioned highest contribution for this source during monsoon season.
509 The principal component representing contribution from biomass could be a composite of multiple sources.
510 Lowest biomass concentration is noted at lorry owner's association petrol pump (location 18). Vehicular
511 emission is identified in the Unmix model and Industrial source by MCR-ALS model. The industrial source

512 is found to contribute higher towards the north of the city and vehicular emission towards the south of the
513 city. Summer season experiences highest contribution from this source and monsoon season the least.

514 Three receptor models (PMF, Unmix and PCA) identified five sources each, while MCR-
515 ALS can only identify three sources (Figure 5). The implementation of MCR-ALS model available
516 in CRAN is designed specifically for spectral analysis, which limits its use in cases where deviation
517 from ideal bilinear behavior is possible. The results from PCA model are unsatisfactory and
518 pollution from most of the sources are attributed to a single source (Crustal) for all three seasons
519 (Figure 4). A KMO sample adequacy of 0.56 is classified as miserable by Henry Kaiser. This
520 would suggest that although some information can be extracted by PCA, the model is ill suited for
521 the data at hand. PMF model did an admirable job in source apportionment of road dust with the
522 detriment that many locations during all three seasons had to be ignored due to them being outliers.
523 Though its performance characteristics are acceptable, the residuals for many species in PMF are
524 considerably greater than all other models in this study. Samples collected from different locations
525 can add uncertainty that is not addressed by PMF model. Of the four models tested, Unmix model
526 is found to give the best source apportionment result, with excellent performance characteristics
527 and lowest scaled residuals of the bunch.

528 **5. Conclusion**

529 Road dust is a significant source of PM in an urban environment. Source apportionment of road dust is thus
530 essential for effectively controlling urban air quality. Receptor models are some of the most robust
531 frameworks available for source apportionment. In this study, the source apportionment performance of
532 four receptor models viz. Unmix, PMF, PCA and MCR-ALS methods are studied and compared. Road dust
533 samples are collected from 18 sampling locations within the study region and analyzed using ICP-OES.
534 The resulting elemental composition data is then used for receptor modeling studies.

535 Unmix model extracted five sources (resuspended dust, tire wear, brake wear, vehicular emission,
536 and crustal material). The PMF model also managed to extract five sources for road dust in the region
537 (vehicular emission, biomass combustion, resuspended dust, and crustal material). Although the PCA
538 method extracted five sources, two sources are found to be of the same composition. The four sources
539 classified by PCA model are crustal material, biomass burning, resuspended dust and vehicular emissions.
540 The MCR-ALS model identified an industrial source, crustal source, and resuspended dust. All four models
541 identified crustal material as the predominant source of road dust in the region. Of the four models tested,
542 UNMIX model is found to give the best results for this dataset.

543 Source apportionment results are expected to be helpful for setting future policy and regulation. This
544 study also brought forth the limitations of different receptor models when applied to road dust. Multivariate
545 receptor models can be immensely powerful tools for controlling and mitigating health effects from urban
546 road dust. More studies comparing the source apportionment performance of receptor models are thus
547 necessary.

548 **Declarations**

549 *Author Contributions*

550 **Jithin Jose:** Conceptualization, Data curation, Methodology, Investigation, Formal Analysis,
551 Software, Validation, Visualization, Writing – original draft. **B. Srimuruganandam:** Project
552 administration, Conceptualization, Methodology, Resources, Supervision, Visualization,
553 Validation, Writing – review & editing.

554 *Funding*

555 The authors have received no specific grant from funding agencies in the public, commercial, or not-for-
556 profit sectors for this research.

557

558 *Compliance with Ethical Standards*

559 The authors declare no conflict of interest.

560 **Acknowledgements**

561 We extend our sincere thanks to Dr. Bhaskar Das, Lab-in-charge, Environmental Engineering Laboratory,
562 School of Civil Engineering, Vellore Institute of Technology, Vellore for offering Microwave digestion
563 and ICP-OES facility. The authors have received no specific grant from funding agencies in the public,
564 commercial, or not-for-profit sectors for this research. The authors declare no conflict of interest.

565 **References**

- 566 Abu-Allaban M, Gillies JA, Gertler AW, et al (2003) Tailpipe, resuspended road dust, and brake-wear
567 emission factors from on-road vehicles. *Atmos Environ* 37:5283–5293.
568 <https://doi.org/10.1016/j.atmosenv.2003.05.005>
- 569 Achad M, Caumo S, de Castro Vasconcellos P, et al (2018) Chemical markers of biomass burning:
570 Determination of levoglucosan, and potassium in size-classified atmospheric aerosols collected in
571 Buenos Aires, Argentina by different analytical techniques. *Microchem J* 139:181–187.
572 <https://doi.org/10.1016/j.microc.2018.02.016>
- 573 Al-Chalabi AS, Hawker D (1997) Response of vehicular lead to the presence of street dust in the Atmos
574 Environ of major roads. *Sci Total Environ* 206:195–202. [https://doi.org/10.1016/S0048-](https://doi.org/10.1016/S0048-9697(97)80010-1)
575 [9697\(97\)80010-1](https://doi.org/10.1016/S0048-9697(97)80010-1)
- 576 Amato F, Pandolfi M, Escrig A, et al (2009) Quantifying road dust resuspension in urban environment by
577 Multilinear Engine: A comparison with PMF2. *Atmos Environ* 43:2770–2780.
578 <https://doi.org/10.1016/j.atmosenv.2009.02.039>
- 579 Amato F, Querol X, Johansson C, et al (2010) A review on the effectiveness of street sweeping, washing
580 and dust suppressants as urban PM control methods. *Sci Total Environ* 408:3070–3084.
581 <https://doi.org/10.1016/j.scitotenv.2010.04.025>
- 582 Andreae MO (1983) Soot Carbon and Excess Fine Potassium: Long-Range Transport of Combustion-
583 Derived Aerosols. *Science* 220:1148–1151. <https://doi.org/10.1126/science.220.4602.1148>
- 584 Arslan H (2001) Heavy Metals in Street Dust in Bursa, Turkey. *J of Trace and Microprobe Tech* 19:439–
585 445. <https://doi.org/10.1081/TMA-100105058>
- 586 ASTM (2001) Standard Test Method for Sieve Analysis of Fine and Coarse Aggregates. In: *Annual Book*
587 *of ASTM Standards*. ASTM, pp 1–5
- 588 Azid A, Juahir H, Ezani E, et al (2015) Identification Source of Variation on Regional Impact of Air Quality
589 Pattern Using Chemometric. *Aerosol Air Qual Res* 15:1545–1558.
590 <https://doi.org/10.4209/aaqr.2014.04.0073>

- 591 Banerjee T, Murari V, Kumar M, Raju MP (2015) Source apportionment of airborne particulates through
592 receptor modeling: Indian scenario. *Atmos Res* 164–165:167–187.
593 <https://doi.org/10.1016/j.atmosres.2015.04.017>
- 594 Bartkowiak A, Dabkowska-Naskret H, Lemanowicz J, Siwik-Ziomek A (2017) Assessment of
595 physiochemical and biological factors of urban street dust. *Environ Prot Eng* 43:155–164.
596 <https://doi.org/10.5277/epe170310>
- 597 Belis CA, Larsen BR, Amato F, et al (2014) European Guide on Air Pollution Source Apportionment with
598 Receptor Models JRC Reference Report. European Union doi: <http://dx.doi.org/10.2788/9332>
- 599 Councell TB, Duckenfield KU, Landa ER, Callender E (2004) Tire-Wear Particles as a Source of Zinc to
600 the Environment. *Environ Sci Technol* 38:4206–4214. <https://doi.org/10.1021/es034631f>
- 601 Das A, Krishna KVSS, Kumar R, et al (2018) Lead isotopic ratios in source apportionment of heavy metals
602 in the street dust of Kolkata, India. *Int J Environ Sci Technol* 15:159–172.
603 <https://doi.org/10.1007/s13762-017-1377-0>
- 604 Devi NL, Yadav IC (2018) Chemometric evaluation of heavy metal pollutions in Patna region of the Ganges
605 alluvial plain, India: implication for source apportionment and health risk assessment. *Environ*
606 *Geochem Hlth* 40:2343–2358. <https://doi.org/10.1007/s10653-018-0101-4>
- 607 Fulton WS (2005) Steel Tire Cord-Rubber Adhesion, Including the Contribution of Cobalt. *Rubber*
608 *Chemistry and Technology* 78:426–457. <https://doi.org/10.5254/1.3547891>
- 609 Galbreath KC, Toman DL, Zygarlicke CJ, et al (2000) Nickel Speciation of Residual Oil Fly Ash and
610 Ambient Particulate Matter Using X-ray Absorption Spectroscopy. *J Air Waste Manag Assoc*
611 50:1876–1886. <https://doi.org/10.1080/10473289.2000.10464230>
- 612 Garg BD, Cadle SH, Mulawa PA, et al (2000) Brake Wear Particulate Matter Emissions. *Environ Sci &*
613 *Technol* 34:4463–4469. <https://doi.org/10.1021/es001108h>
- 614 Glover I (1966) The Fuel Additive Approach Towards the Alleviation of the Nuisance of Diesel Smoke.
615 The Institute of Petroleum
- 616 Gramstat S (2018) Chapter 10 - Technological Measures for Brake Wear Emission Reduction: Possible
617 Improvement in Compositions and Technological Remediation: Cost Efficiency. *Non-Exhaust*
618 *Emissions* 205–227. <https://doi.org/10.1016/B978-0-12-811770-5.00010-8>
- 619 Habibi Kamran (1970) Characterization of particulate lead in vehicle exhaust-experimental techniques.
620 *Environ Sci Technol* 4:239–248. <https://doi.org/10.1021/es60038a001>
- 621 Henry RC (1991) *Multivariate receptor models*. Elsevier Science Publishers, Amsterdam
- 622 Henry RC (2003) Multivariate receptor modeling by N-dimensional edge detection. *Chemom Intell Lab*
623 *Syst* 65:179–189. [https://doi.org/10.1016/S0169-7439\(02\)00108-9](https://doi.org/10.1016/S0169-7439(02)00108-9)
- 624 Henry RC, Lewis CW, Hopke PK, Williamson HJ (1984) Review of receptor model fundamentals. *Atmos*
625 *Environ* (1967) 18:1507–1515. [https://doi.org/10.1016/0004-6981\(84\)90375-5](https://doi.org/10.1016/0004-6981(84)90375-5)
- 626 Heo J-B, Hopke PK, Yi SM (2009) Source apportionment of PM 2.5 in Seoul, Korea. *Atmospheric Chem*
627 *Phys* 9:4957–4971. <https://doi.org/10.5194/acp-9-4957-2009>
- 628 Hermant M, Basset D, Razet JC (1986) Lubricant compositions containing calcium and barium fluorides
- 629 Hilden DL, Bergin SP (1986) The Effect of Manganese Fuel Additive and Exhaust Gas Recirculation on
630 Diesel Particulate Emissions. *SAE Transactions* 95:250–269. <https://doi.org/10.4271/860621>
- 631 Hopke PK (2016) Review of receptor modeling methods for source apportionment. *J Air Waste Manag*
632 *Assoc* 66:237–259. <https://doi.org/10.1080/10962247.2016.1140693>

- 633 IARC (2020) List of Classifications – IARC Monographs on the Identification of Carcinogenic Hazards to
634 Humans. <https://monographs.iarc.fr/list-of-classifications>. Accessed 13 May 2020
- 635 Isaac CPJ, Sivakumar A, Kumar CRP (2012) Lead levels in breast milk, blood plasma and intelligence
636 quotient: a health hazard for women and infants. *Bull environ contam toxicol* 88:145–149
- 637 Johnson TM, Guttikunda S, et al (2011) A Review of Top-down Source Apportionment Techniques and
638 Their Application in Developing Countries. The World Bank Group.
- 639 Jose J, Srimuruganandam B (2020) Investigation of road dust characteristics and its associated health risks
640 from an urban environment. *Environ Geochem Hlth*. <https://doi.org/10.1007/s10653-020-00521-6>
- 641 Khpalwak W, Jadoon WA, Abdel-dayem SM, Sakugawa H (2019) Polycyclic aromatic hydrocarbons in
642 urban road dust, Afghanistan: Implications for human health. *Chemosphere* 218:517–526.
643 <https://doi.org/10.1016/j.chemosphere.2018.11.087>
- 644 Konstandopoulos AG, Gratz LD, Johnson JH, et al (1988) Ceramic Particulate Traps for Diesel Emissions
645 Control — Effects of a Manganese–Copper Fuel Additive. *SAE Trans* 97:37–53
- 646 Kukutschová J, Filip P (2018) Chapter 6 - Review of Brake Wear Emissions: A Review of Brake Emission
647 Measurement Studies: Identification of Gaps and Future Needs. *Non-Exhaust Emissions* 123–146.
648 <https://doi.org/10.1016/B978-0-12-811770-5.00006-6>
- 649 Kupiainen KJ, Tervahattu H, Räsänen M, et al (2005) Size and Composition of Airborne Particles from
650 Pavement Wear, Tires, and Traction Sanding. *Environ Sci Technol* 39:699–706.
651 <https://doi.org/10.1021/es035419e>
- 652 Lakshminarayanan PA, Nayak NS (2011) Critical Component Wear in Heavy Duty Engines. John Wiley
653 & Sons
- 654 Mao Y, Wilson JD, Kort J (2013) Effects of a shelterbelt on road dust dispersion. *Atmos Environ* 79:590–
655 598. <https://doi.org/10.1016/j.atmosenv.2013.07.015>
- 656 Marín MRP, Gil EP, Blázquez LC, Capelo-Martínez JL (2011) Determination of trace and major elemental
657 profiles in street dust samples by fast miniaturized ultrasonic probe extraction and ICP-MS. *Talanta*
658 84:840–845. <https://doi.org/10.1016/j.talanta.2011.02.012>
- 659 MHRD (2015) Re classification of cities/towns on the basis of census-2011 for the purpose of grant of HRA
660 to central government. New Delhi
- 661 Miguel AG, Cass GR, Glovsky MM, Weiss J (1999) Allergens in Paved Road Dust and Airborne Particles.
662 *Environ Sci Technol* 33:4159–4168. <https://doi.org/10.1021/es9904890>
- 663 Monaci F, Bargagli R (1997) Barium and Other Trace Metals as Indicators of Vehicle Emissions. *Water*
664 *Air Soil Poll* 100:89–98. <https://doi.org/10.1023/A:1018318427017>
- 665 Monaci F, Moni F, Lanciotti E, et al (2000) Biomonitoring of airborne metals in urban environments: new
666 tracers of vehicle emission, in place of lead. *Environ Poll* 107:321–327.
667 [https://doi.org/10.1016/S0269-7491\(99\)00175-X](https://doi.org/10.1016/S0269-7491(99)00175-X)
- 668 Ooij WJ van (1984) Mechanism and Theories of Rubber Adhesion to Steel Tire Cords—An Overview.
669 *Rubber Chem Technol* 57:421–456. <https://doi.org/10.5254/1.3536016>
- 670 Paatero P, Tapper U (1994) Positive matrix factorization: A non-negative factor model with optimal
671 utilization of error estimates of data values. *Environmetrics* 5:111–126.
672 <https://doi.org/10.1002/env.3170050203>
- 673 Pant P, Harrison RM (2012) Critical review of receptor modelling for particulate matter: A case study of
674 India. *Atmos Environ* 49:1–12. <https://doi.org/10.1016/j.atmosenv.2011.11.060>

- 675 Peltier RE, Hsu S-I, Lall R, Lippmann M (2009) Residual oil combustion: a major source of airborne nickel
676 in New York City. *J Expo Sci Environ Epidemiol* 19:603–612. <https://doi.org/10.1038/jes.2008.60>
- 677 Pio CA, Legrand M, Alves CA, et al (2008) Chemical composition of atmospheric aerosols during the 2003
678 summer intense forest fire period. *Atmos Environ* 42:7530–7543.
679 <https://doi.org/10.1016/j.atmosenv.2008.05.032>
- 680 Rastegar F, Craft AE (1993) Piston ring coatings for high horsepower diesel engines. *Surf Coat Technol*
681 61:36–42. [https://doi.org/10.1016/0257-8972\(93\)90199-X](https://doi.org/10.1016/0257-8972(93)90199-X)
- 682 Rudnick RL, Shaner A, Portillo K (2019) Top 5 elements in the upper crust of Earth. Top five elements in
683 the upper crust of Earth
- 684 Sharma R, Pervez S (2003) Enrichment and Exposure of Particulate Lead in a Traffic Environment in India.
685 *Environ Geochem Hlth* 25:297–306. <https://doi.org/10.1023/A:1024520522083>
- 686 Tauler R, Viana M, Querol X, et al (2009) Comparison of the results obtained by four receptor modelling
687 methods in aerosol source apportionment studies. *Atmos Environ* 43:3989–3997.
688 <https://doi.org/10.1016/j.atmosenv.2009.05.018>
- 689 Taylor SR (1964) Abundance of chemical elements in the continental crust: a new table. *Geochim*
690 *Cosmochim Acta* 28:1273–1285. [https://doi.org/10.1016/0016-7037\(64\)90129-2](https://doi.org/10.1016/0016-7037(64)90129-2)
- 691 Testa SM (2004) Sources of Chromium Contamination in Soil and Groundwater. In: *Chromium(VI)*
692 *Handbook*. CRC Press
- 693 Thomaidis NS, Bakeas EB, Siskos PA (2003) Characterization of lead, cadmium, arsenic and nickel in
694 PM_{2.5} particles in the Athens atmosphere, Greece. *Chemosphere* 52:959–966.
695 [https://doi.org/10.1016/S0045-6535\(03\)00295-9](https://doi.org/10.1016/S0045-6535(03)00295-9)
- 696 Thorpe A, Harrison RM (2008) Sources and properties of non-exhaust particulate matter from road traffic:
697 A review. *Sci Total Environ* 400:270–282. <https://doi.org/10.1016/j.scitotenv.2008.06.007>
- 698 Thurston GD, Spengler JD (1985) A multivariate assessment of meteorological influences on inhalable
699 particle source impacts. *J Clim Appl Meteorol* 24:1245–1256
- 700 Truex TJ, Pierson WR, McKee DE, et al (1980) Effects of barium fuel additive and fuel sulfur level on
701 diesel particulate emissions. *Environ Sci Technol* 14:1121–1124
- 702 Turekian KK, Wedepohl KH (1961) Distribution of the Elements in Some Major Units of the Earth's Crust.
703 *GSA Bull* 72:175–192. [https://doi.org/10.1130/0016-7606\(1961\)72\[175:DOTEIS\]2.0.CO;2](https://doi.org/10.1130/0016-7606(1961)72[175:DOTEIS]2.0.CO;2)
- 704 U.S. EPA O (1996) EPA Method 3050B: Acid Digestion of Sediments, Sludges, and Soils
- 705 Wang C-F, Chang C-Y, Tsai S-F, Chiang H-L (2005) Characteristics of Road Dust from Different Sampling
706 Sites in Northern Taiwan. *J Air Waste Manag Assoc* 55:1236–1244.
707 <https://doi.org/10.1080/10473289.2005.10464717>
- 708 Xie M, Teresa LC, et al. Intra-Urban Spatial Variability and Uncertainty Assessment of PM_{2.5} Sources
709 Based on Carbonaceous Species. *Atmos Environ* 60:305–15.
710 <https://doi.org/10.1016/j.atmosenv.2012.06.036>.
- 711 Yaroshevsky AA (2006) Abundances of chemical elements in the Earth's crust. *Geochem Int* 44:48–55.
712 <https://doi.org/10.1134/S001670290601006X>
- 713 Yasuda T, Kondo H, Echigo Y, et al (1990) Rubber compositions for tires
- 714 Yu J, Yan C, Liu Y, et al (2018) Potassium: A Tracer for Biomass Burning in Beijing? *Aerosol Air Qual*
715 *Res* 18:2447-2459. <https://doi.org/10.4209/aaqr.2017.11.0536>

716 Zeng X, Xu X, Qin Q, et al (2019) Heavy metal exposure has adverse effects on the growth and development
717 of preschool children. *Environ Geochem Hlth* 41:309–321. [https://doi.org/10.1007/s10653-018-](https://doi.org/10.1007/s10653-018-0114-z)
718 0114-z

719 Zhang Y, Cai J, Wang S, et al (2017) Review of receptor-based source apportionment research of fine
720 particulate matter and its challenges in China. *Sci Total Environ* 586:917-929.
721 <https://doi.org/10.1016/j.scitotenv.2017.02.071>

722

723

724

725

726

727

728

729

730

731

732

733

734

735

736

737

738 **Figures**

739 Figure 1: Sampling locations

740 Figure 2: Source contribution in study locations (above) and source contribution by elements (below) from
741 the Unmix model

742 Figure 3: Source contribution in study locations (above) and source contribution by elements (below) from
743 the PMF model

744 Figure 4: Source contribution in study locations (above) and source contribution by elements (below) from
745 the PCA model

746 Figure 5: Source contribution in study locations (above) and source contribution by elements (below) from
747 the MCR model

748 Figure 6: Distribution of sources in the study region. Lines represent the contribution of individual sources
749 as calculated by different receptor models. Map on the right shows the different sampling
750 locations. Explanation of sampling locations is provided in Table 1. (units in % contribution)

751 **Tables**

752 Table 1: List of sampling locations

753 Table 2: Principal component scores from PCA analysis (significant values are in bold)

754 **Supplementary Tables**

755 Table S1: Mean and SD of elements from input data (Generated by Unmix model)

756 Table S2: Unmix Source composition (units in mg/kg)

757 Table S3: Unmix Source contribution (units in mg/kg)

- 758 Table S4: Correlation between unmix models
- 759 Table S5: Scaled residuals from Unmix model
- 760 Table S6: PMF Source contribution (no contribution shown by -999)
- 761 Table S7: PMF Source composition (units in mg/kg)
- 762 Table S8: Source contribution from PCA model
- 763 Table S9: Source loading from MCR-ALS
- 764 Table S10: Source contribution from MCR-ALS
- 765 Table S11: Scaled residuals from MCR-ALS model
- 766 Table S12: Residuals for PMF model

Figures

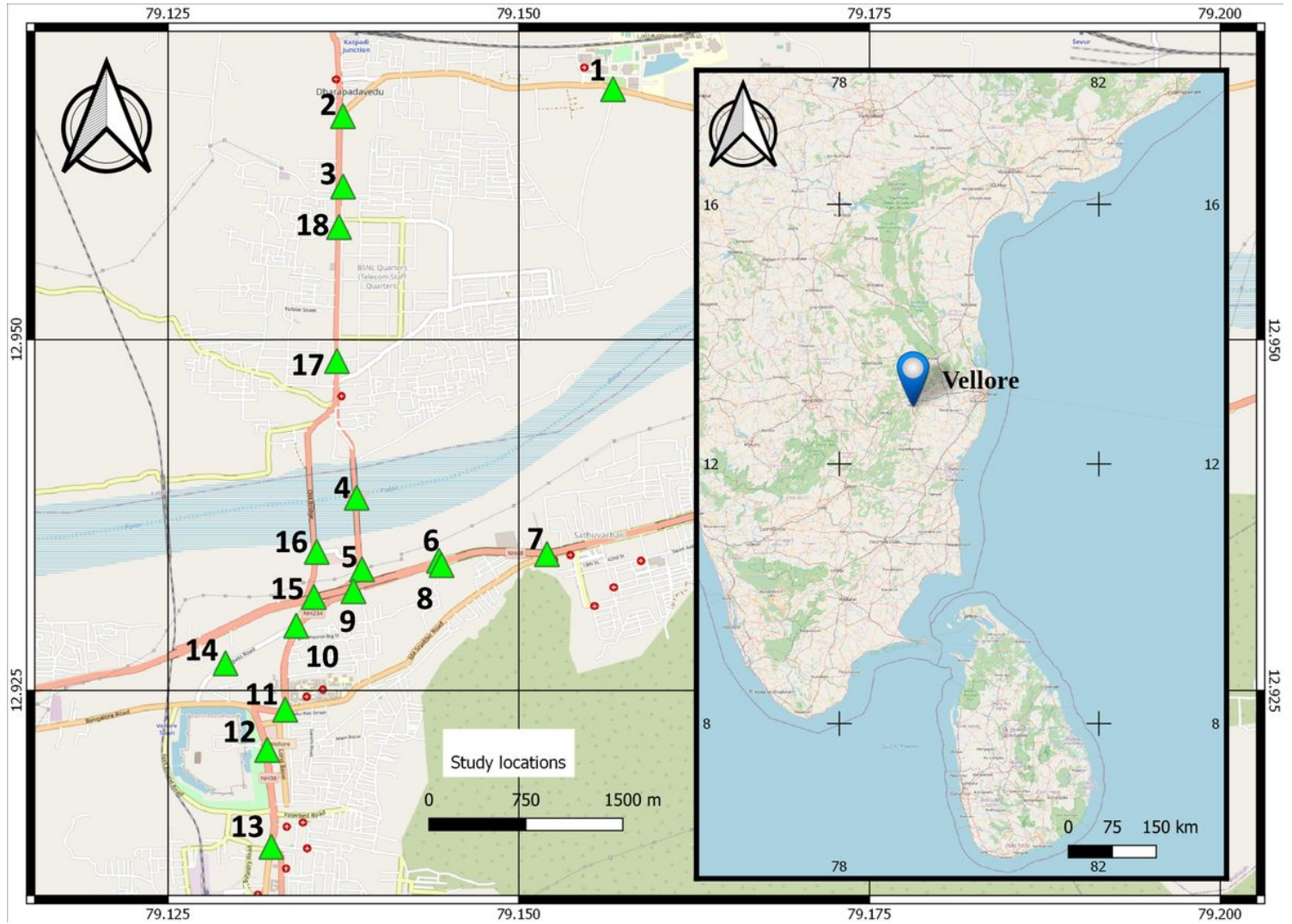


Figure 1

Sampling locations

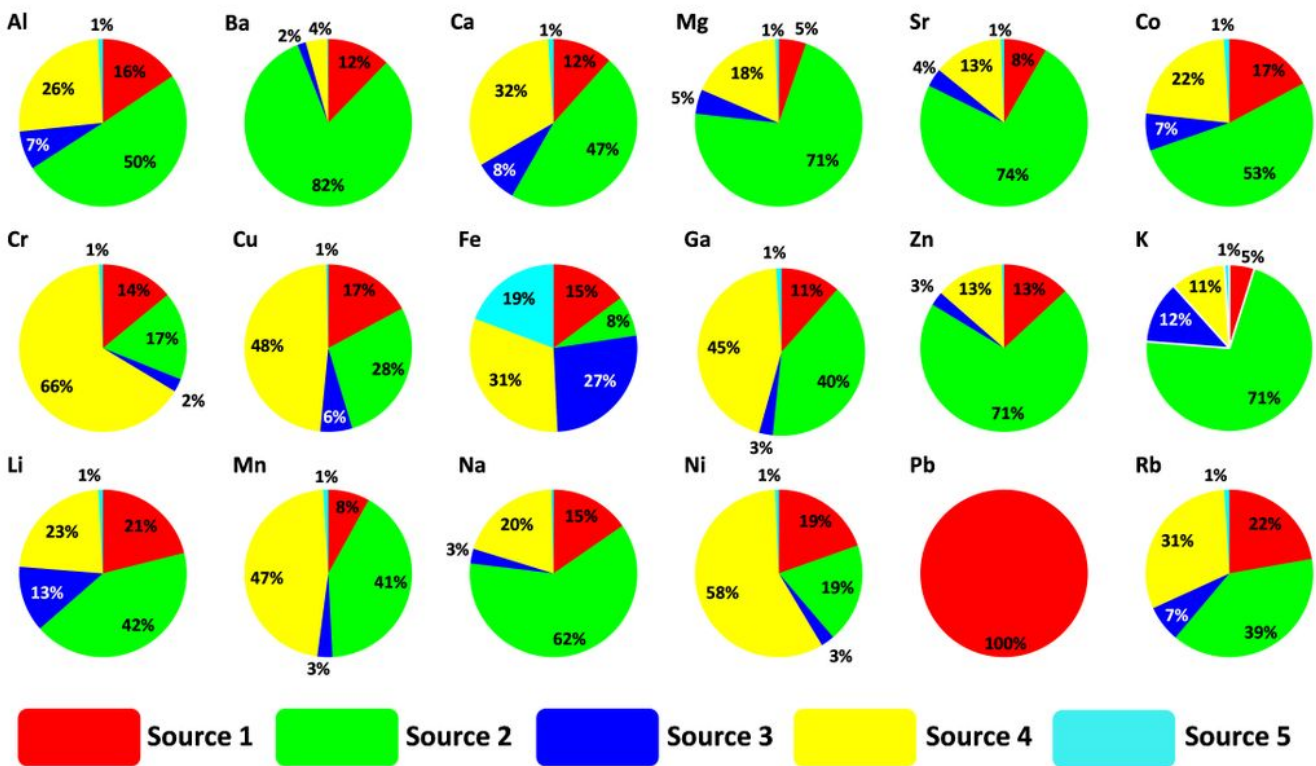
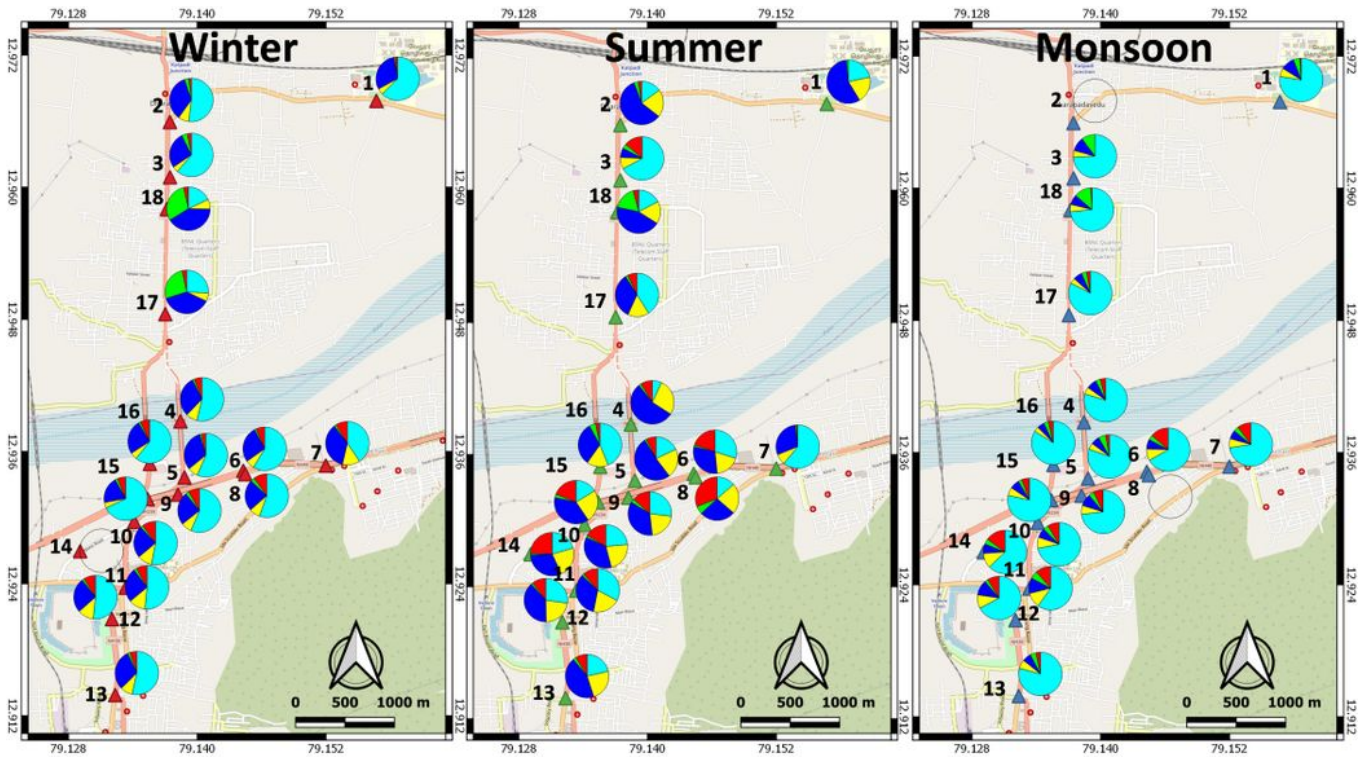


Figure 2

Source contribution in study locations (above) and source contribution by elements (below) from the Unmix model

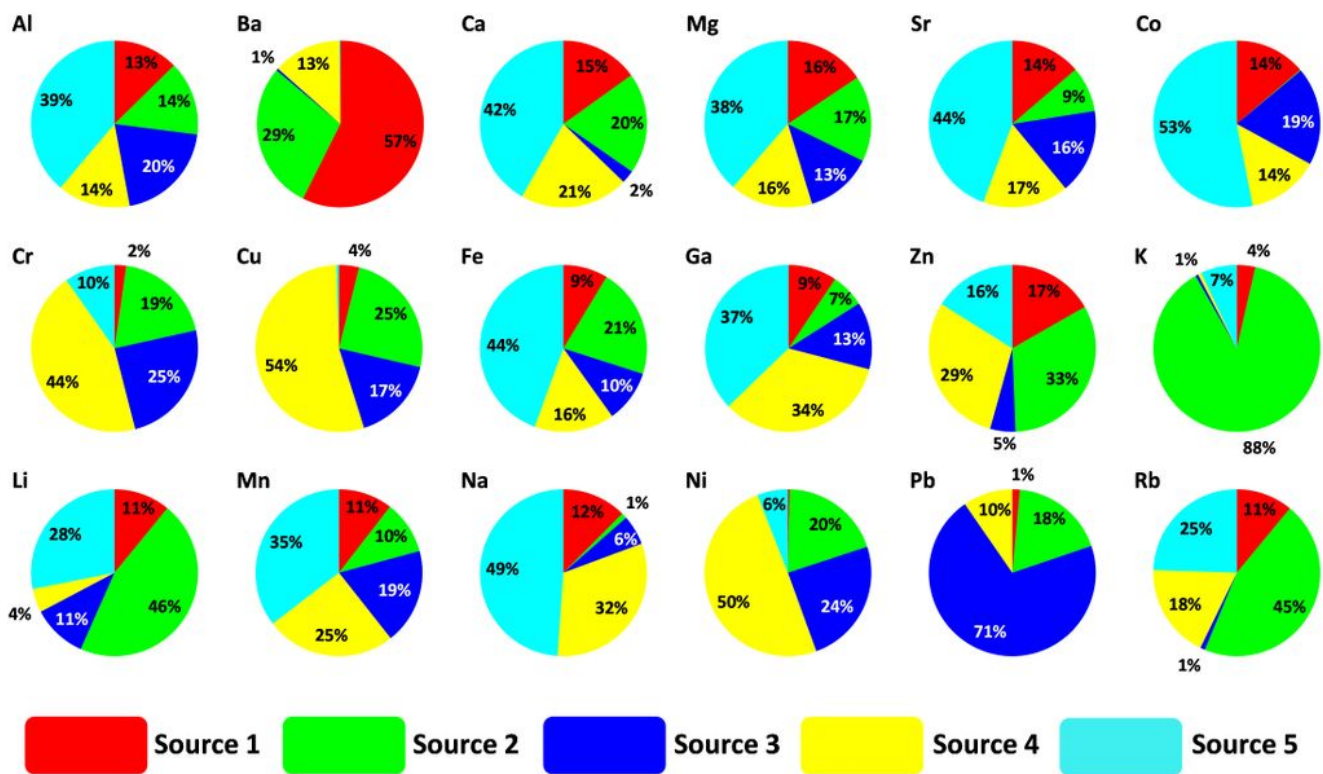
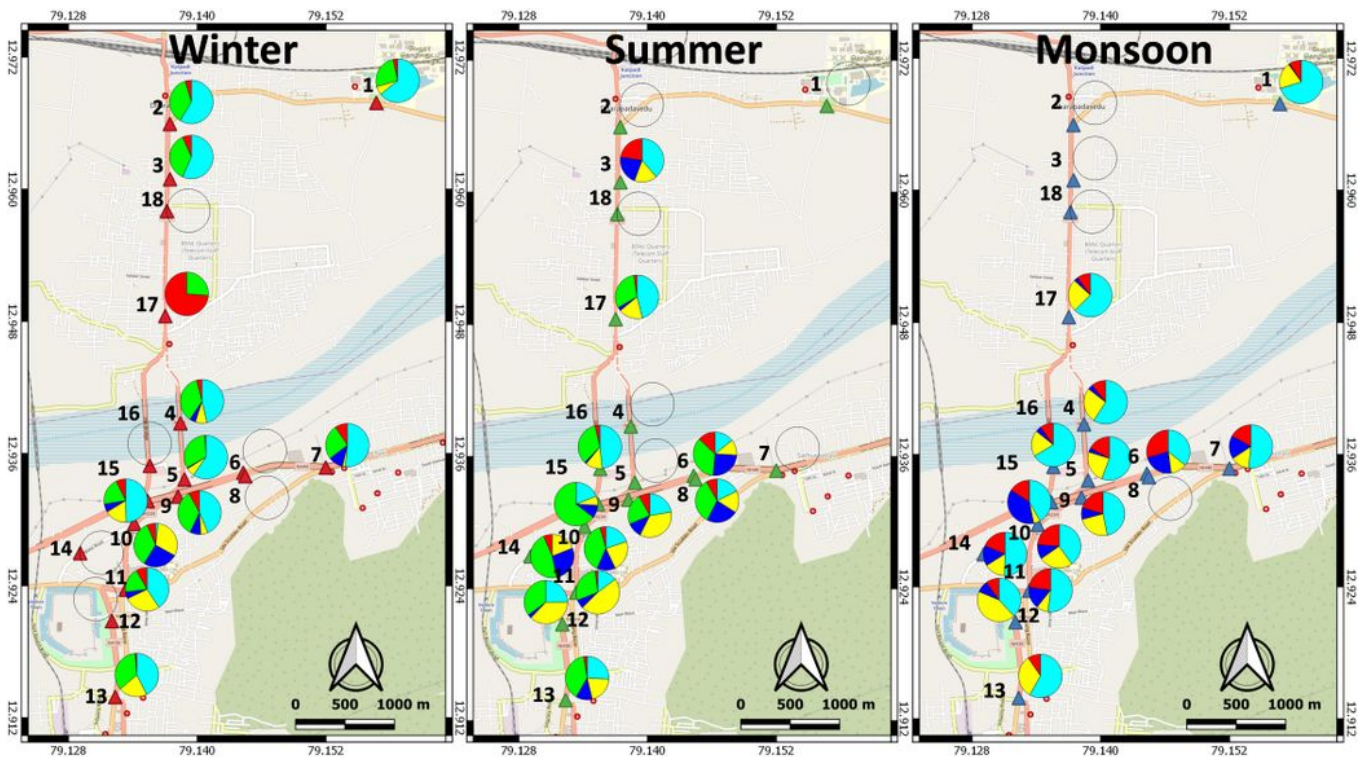


Figure 3

Source contribution in study locations (above) and source contribution by elements (below) from the PMF model

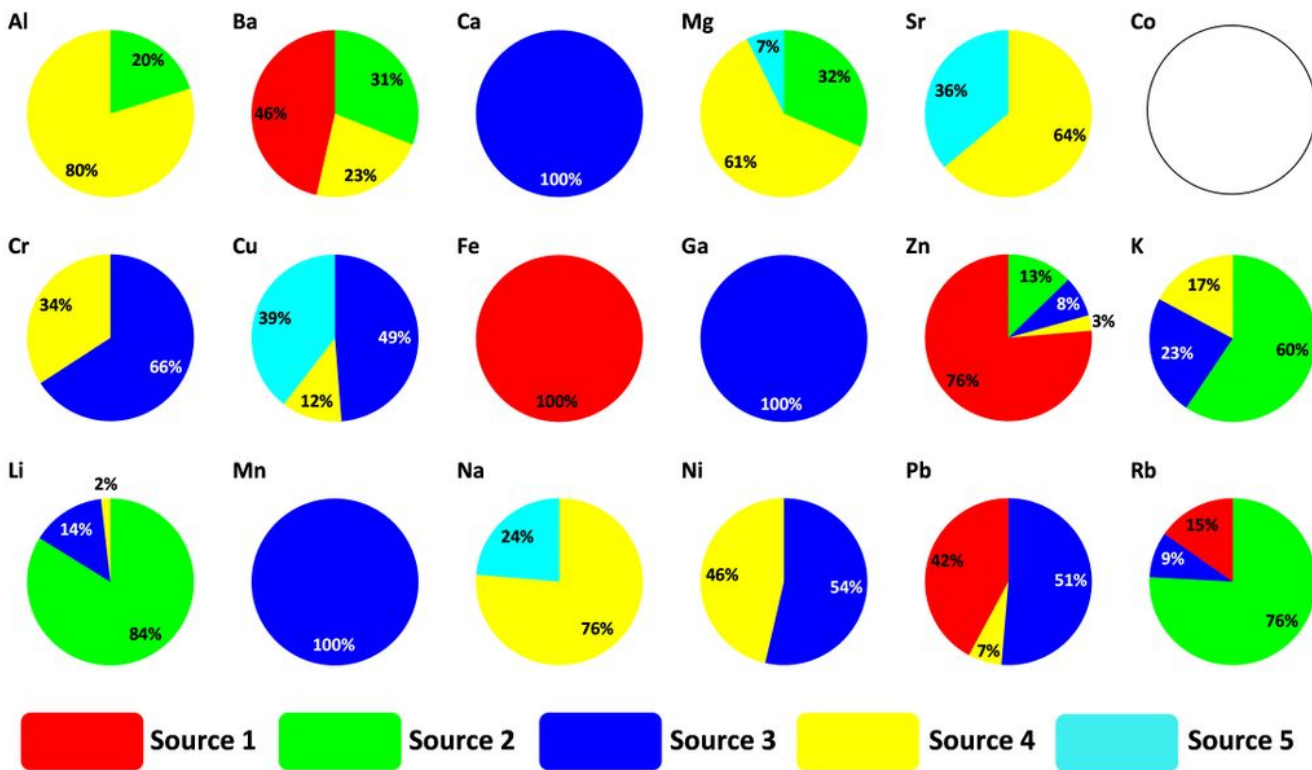
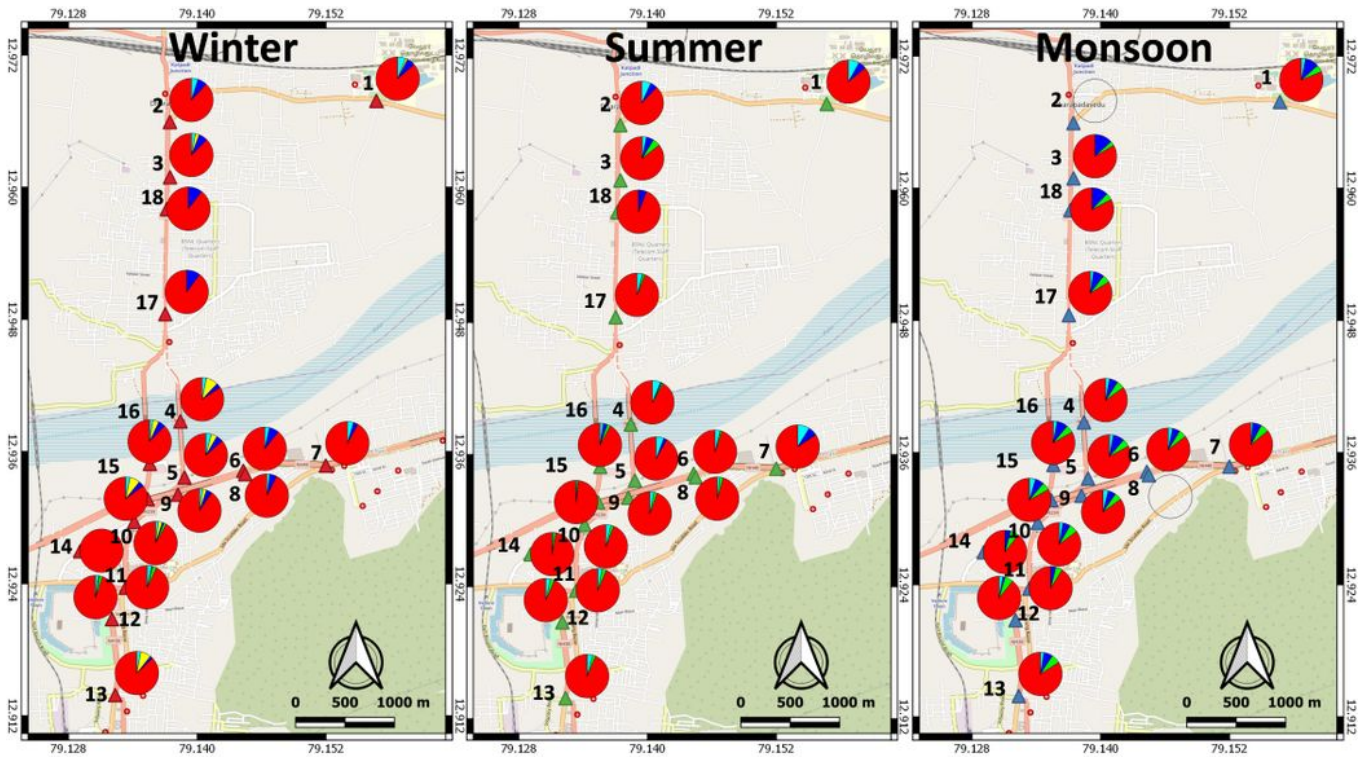


Figure 4

Source contribution in study locations (above) and source contribution by elements (below) from the PCA model

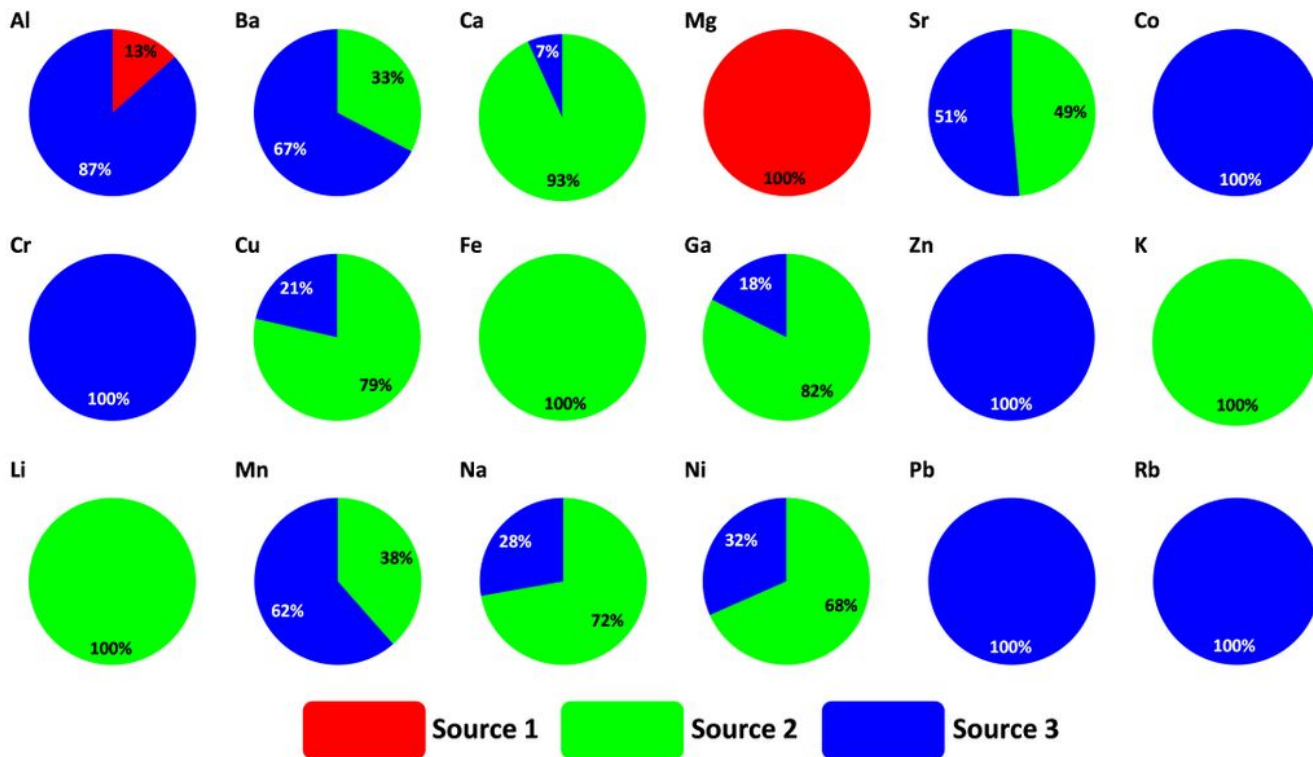
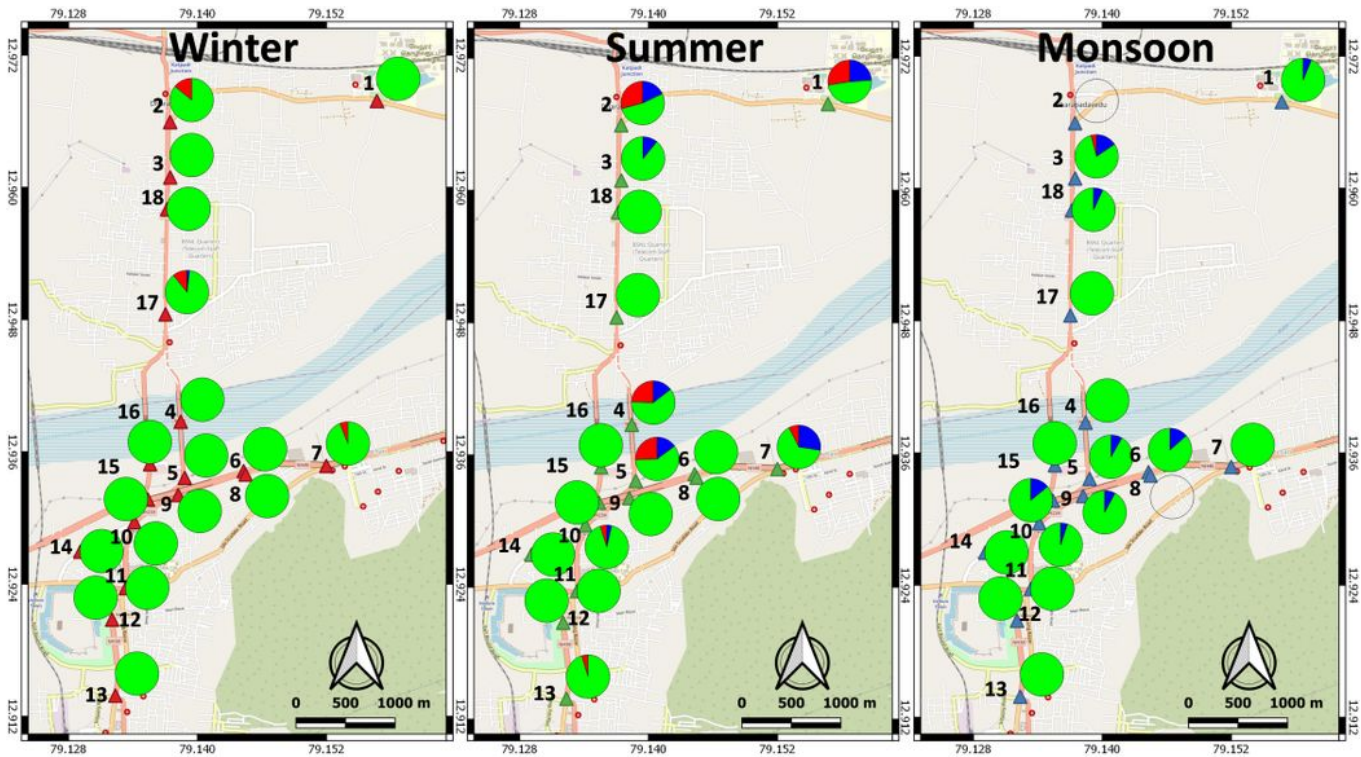


Figure 5

Source contribution in study locations (above) and source contribution by elements (below) from the MCR model

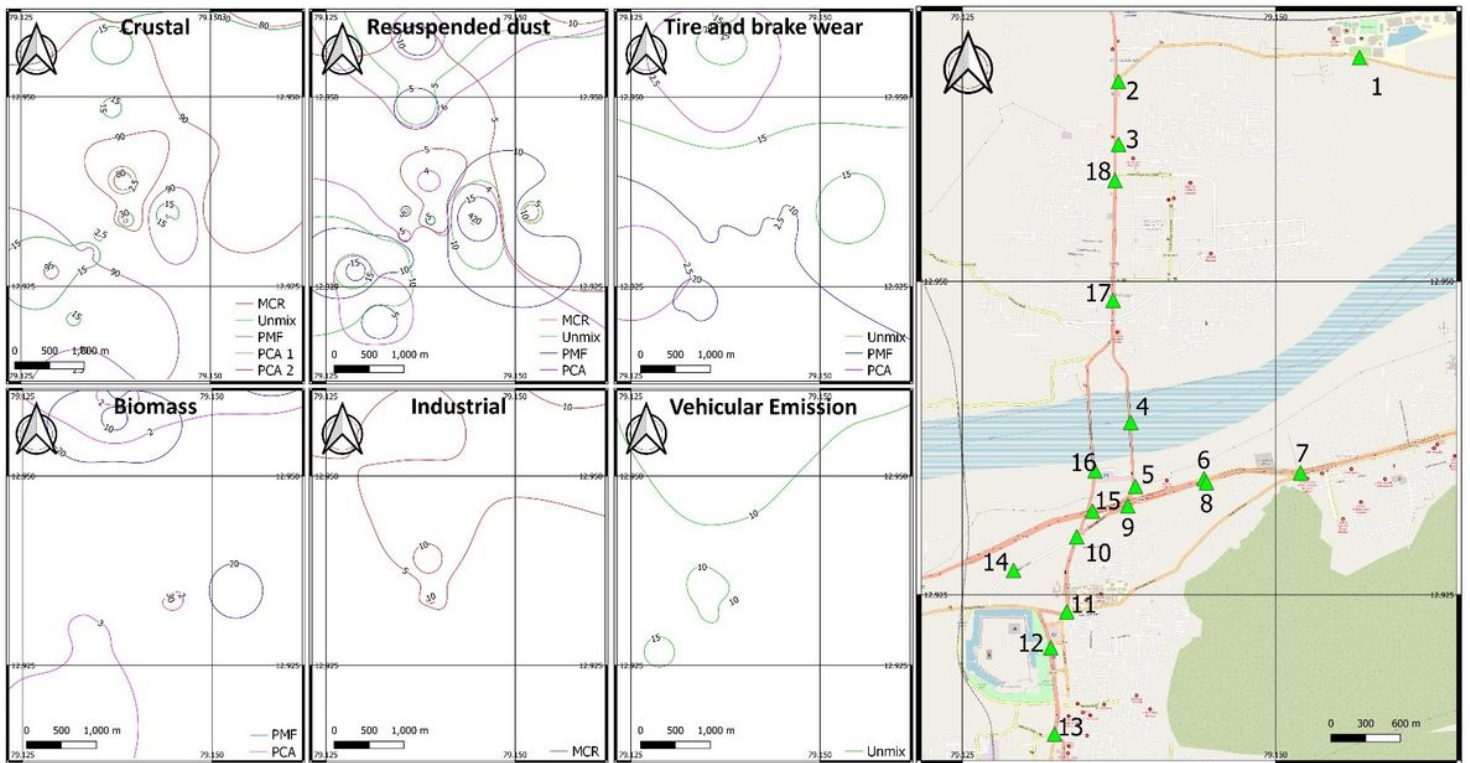


Figure 6

Distribution of sources in the study region. Lines represent the contribution of individual sources as calculated by different receptor models. Map on the right shows the different sampling locations. Explanation of sampling locations is provided in Table 1. (Units in % contribution)

Supplementary Files

This is a list of supplementary files associated with this preprint. Click to download.

- [TableS1.docx](#)
- [TableS2.docx](#)
- [TableS3.docx](#)
- [TableS4.docx](#)
- [TableS5.docx](#)
- [TableS6.docx](#)
- [TableS7.docx](#)
- [TableS8.docx](#)
- [TableS9.docx](#)
- [TableS10.docx](#)
- [TableS11.docx](#)

- [TableS12.docx](#)